JOURNAL OF MATERIALS SCIENCE 23 (1988) 2230–2242

Fractal analysis of rubber wear surfaces and debris

P. R. STUPAK, J. A. DONOVAN
Mechanical Engineering, University of Massachusetts, Amherst, Massachusetts 01003, USA

The wear surface and debris of three rubber compounds (NR, PBD and NR/PBD/SBR), worn on a modified blade abrader, were fractal. The fractal dimension of the wear surface was: (1) limited to a finite range, and if the wear mechanism remained the same; (2) independent of the wear load; and (3) the basis for creating a master fractal plot by a shift factor that (4) decreased linearly with wear load. The fractal dimension of wear was determined on the basis of profilometer traces and showed that the wear load affected the scale of the wear process. The fractal dimension of the debris also increased with the wear load and is thought to be a function of the agglomeration mechanism during wear.

1. Introduction

To appreciate the practical nature of rubber wear, one need only consider that an estimated 430 Gg of rubber are lost through tyre wear in the United States annually [1]. Past advances in rubber wear properties were achieved chiefly through empirical relations and expensive road testing [2]. But, diminishing resources and increased competition require future improvements to be gained by a more effective method based on the understanding of the mechanisms of wear. This undertaking is difficult because of the complexity of the wear phenomenon which currently is thought to include tensile, fatigue, mechanochemical, thermochemical, and oxidative processes [3]. However, lasting evidence of these processes is found through the examination of the remaining wear surfaces and debris.

1.1. Rubber wear

For example, the overt signs of wear for many rubber compounds are surface roughening and the formation of small particles known as primary wear debris. Wear is due to frictional forces between an asperity and the rubber surface causing the rupture of primary molecular bonds [4]. Continued wear in one direction results in the formation of ridges perpendicular to the direction of motion. Eventually the pattern of ridges attain a steady state size and spacing, and the wear rate is constant. A microscopic survey of worn tyre tread by Smith and Veith [5] reported that the easily visible pattern consisted of several levels of even smaller ridges upon magnification. This process of ridge formation was originally recognized by Shallamach [6] as being fatigue dominated. Later, Thomas [7] and Southern and Thomas [8] supported this view by developing a fatigue model of steady state wear based on fracture mechanics concepts. More recently, however, Gent and Pulford [2] and Zhang [9] have shown that wear involves tensile failure and chemical effects as well as fatigue.

However, the dry wear mode described above does not occur in all materials at all times. When certain compounds are worn under mild conditions, reactive species generated by the rupture of rubber molecules react with oxygen in the atmosphere to form a degraded product. This is called oily mode wear because a thin oily film eventually covers the surface and reduces the rate of wear [2]. Ridges which may have been present initially are rounded and the complex surface altered [9].

In the past, studies [2, 8, 9] of rubber wear topography have shown that the spacing between ridges and the size of the wear debris are proportional to the applied frictional force under dry wear conditions. An improved method of surface and debris analysis which distinguishes wear mechanisms and correlates with wear properties would be useful in helping select rubber compounds for service. To this end, this study analysed profilometry traces of worn surfaces and boundary profiles of wear debris by fractal concepts. Fractal plots correlated with wear mechanism, wear rate and frictional work.

1.2. Fractal geometry

Fractal analysis, created by Mandelbrot [10], can be thought of as a tool which produces a quantitative description of an otherwise indescribably rugged line or surface. The essence of fractal analysis is: the length (or area) of an irregular line (or surface) depends on the size of the measuring device. Small measuring devices resolve finer details than larger, thereby give greater length (or area) measurements. A graphical representation of log length (L) of a mathematical fractal curve against log measuring unit size (R) yields a straight line described by the relation

$$L \propto R^{(1-D)} \tag{1}$$

where D is the fractal dimension. For example, a smooth line gives a constant length for all measuring unit lengths; the resulting fractal dimension equals the Euclidian dimension of one for a line. However, D for

0022–2461/88 $03.00 + .12

an irregular line is greater than one and increases with increasing roughness to a limit of two.

An analogous expression for complex surfaces produces fractal dimensions ranging from the Euclidean $D = 2$ to $D = 3$.

The length estimate continually increases because a mathematically fractal object posesses self-similarity. That is, every large irregularity is composed of smaller irregularities. Mathematical fractals possess self-similarity at all length scales, but natural fractal objects are always limited by upper and lower bounds [10].

Applications of fractal geometry have ranged from interpreting the irregular nature of clouds [11] to the description of Brownian motion [10]. Recently, several authors have determined the fractal dimensions of metal fracture surfaces. In a study by Mandelbrot *et al.* [12], of 300 grade maraging steel as a function of heat treatment, the fracture surfaces were first nickel plated and then polished parallel to the fracture plane in several stages. Each stage revealed a set of irregular "islands" of the underlying steel. The relation of the island area, A, to its perimeter, P, for many islands was

$$P \propto A^{(D/2)} \tag{2}$$

and D decreased with the impact energy required to fracture the specimen; a result which appears counter-intuitive [13].

Two other investigations [13, 14] determined D by applying Equation 1 to micrographs of polished vertical sections of the metal fracture surfaces. The study by Underwood and Banerji [14] showed that fracture surfaces are generally self-similar over only a limited range of scale.

2. Wear testing

2.1. Experimental methods

Wear testing was performed with a modified blade abrader [7, 9]. Wear proceeds by forcing a rigid stationary razor blade into the circumferential surface of a rotating rubber wheel. The stiff cantilever beam holding the blade was instrumented with strain gauges to record the transverse frictional forces generated during wear.

Three rubber compounds (Table I) were tested under frictional forces ranging from 650 to 2150 N per metre of wheel width, which corresponds to a frictional work input of 650 to 2150 J per square metre of nominal wheel surface area. All compounds were tested at 25° C and a tangential velocity of 33 mm sec^{-1} to minimize the effect of frictional heating on the wear rate. In addition, wear measurements were made only after each sample formed a steady state wear pattern. A nylon brush continually removed wear particles during testing. The wear rate was determined from rubber weight loss, testing time, r.p.m., compound density, and was expressed as the decrease in the radial wheel thickness per revolution. After testing, the specimens and collected debris were stored in a desiccator to prevent absorption of moisture and oxidation.

TABLE I Compound formulations

Formulation	NR compound	Blend compound	PBD compound
NR	100	0.33	0.0
PBD	0.0	0.33	100.0
SBR	0.0	0.33	0.0
Zinc oxide	4.0		4.0
Steric acid	2.0		2.0
Black, N110	45.0		45.0
Agerite Resin D	0.5		0.5
Agerite White	0.5		0.5
Anozite 2	3.0		3.0
Sulphur	2.5		2.0
Stanocure	0.8		1.5
Cure (min/° F)	25/300		20/300

2.2. Results and discussion

The radial wear rate as a function of frictional work input is shown in Fig. 1 for the three compounds. The data conform to the same relation found in experiments by Thomas [7], Gent [2], and Zhang [9]

$$W = AF^n \tag{3}$$

where W is the radial wear rate, F the applied frictional work input, and A and n are material parameters and are listed in Table II.

The least wear resistant material was the natural rubber (NR) compound. All NR samples tested developed steady state wear patterns and produced non-adhering particulate debris indicative of the dry wear mode. The ridge height, spacing, and debris size increased with increasing frictional work input (Fig. 2).

The natural rubber, polybutadiene, and styrene butadiene blend compound (NR, PBD, and SBR Blend) ranked second. Samples run at work inputs greater than 1100 J m^{-2} formed steady state ridges similar in size to the NR material, but produced strongly adhering rolls of debris. Brushing would not remove the debris so the testing was periodically interrupted to pull the particles from the surface with tweezers. At work inputs below 1100 J m^{-2}, ridge formation associated with dry wear occurred initially, but soon transformed into the oily wear mode. A dark, oily film formed, rounding the existing ridges and decreasing the wear rate to an unmeasurably low level (Fig. 3).

The PBD compound wore in the dry mode only and was the most abrasion resistant material. The scale of the ridges and the debris were much finer than the other compounds. As with the other dry wear samples, the pattern height, spacing, and debris size increased with increasing frictional work input (Fig. 4).

3. Profilometry

3.1. Experimental details

A traversing Clevite Surfanalyser 150 profilometer recorded surface roughness profiles in the rotation direction. For each compound, traces were made of samples worn at several different frictional work inputs. Traces were obtained at five or six locations around the wheel circumference to develop a statistical representation of the surface. The forward and reverse trace of each location was recorded for

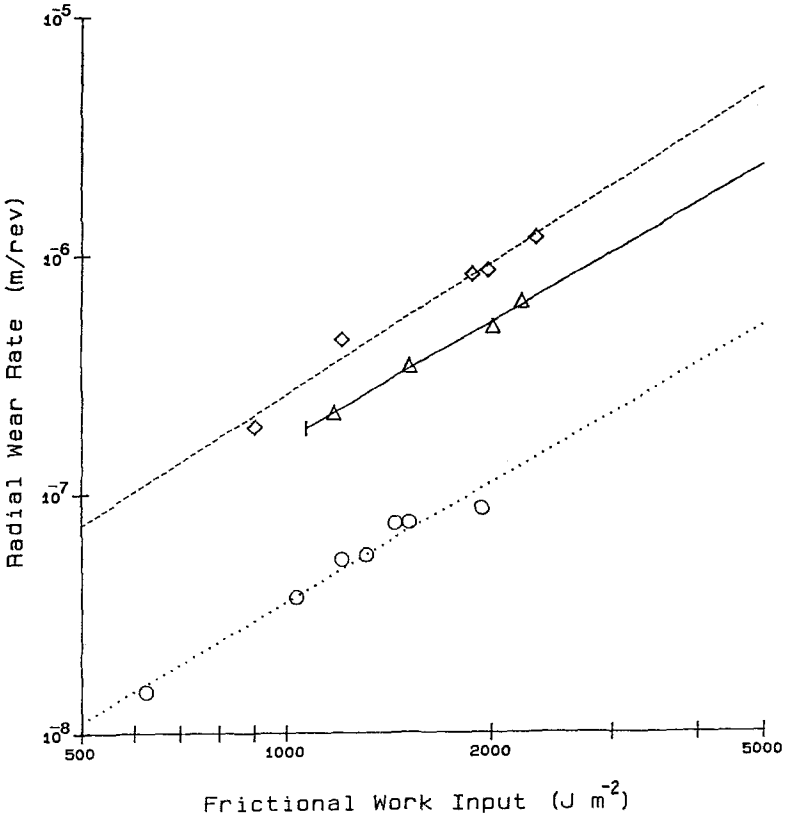

Figure 1 Radial wear rate as a function of frictional work input. (△) Blend, (◇) NR, (○) PBD.

analysis to include differences of roughness observed by the stylus deforming some of the thin ridge tips. Additionally, a vertical to horizontal enhancement of ten to one was used in all cases. The amplification of the roughness allowed more accurate analysis because even very small features became measurable. The total circumferential trace length for each sample was approximately 3 cm. The ability of the profilometer to form a consistent detailed surface representation over such a large distance was the reason for its use in this study. A microscopic survey of surface cross-sections at the same resolution, while giving a more exact surface description, would require a prohibitive number of micrographs.

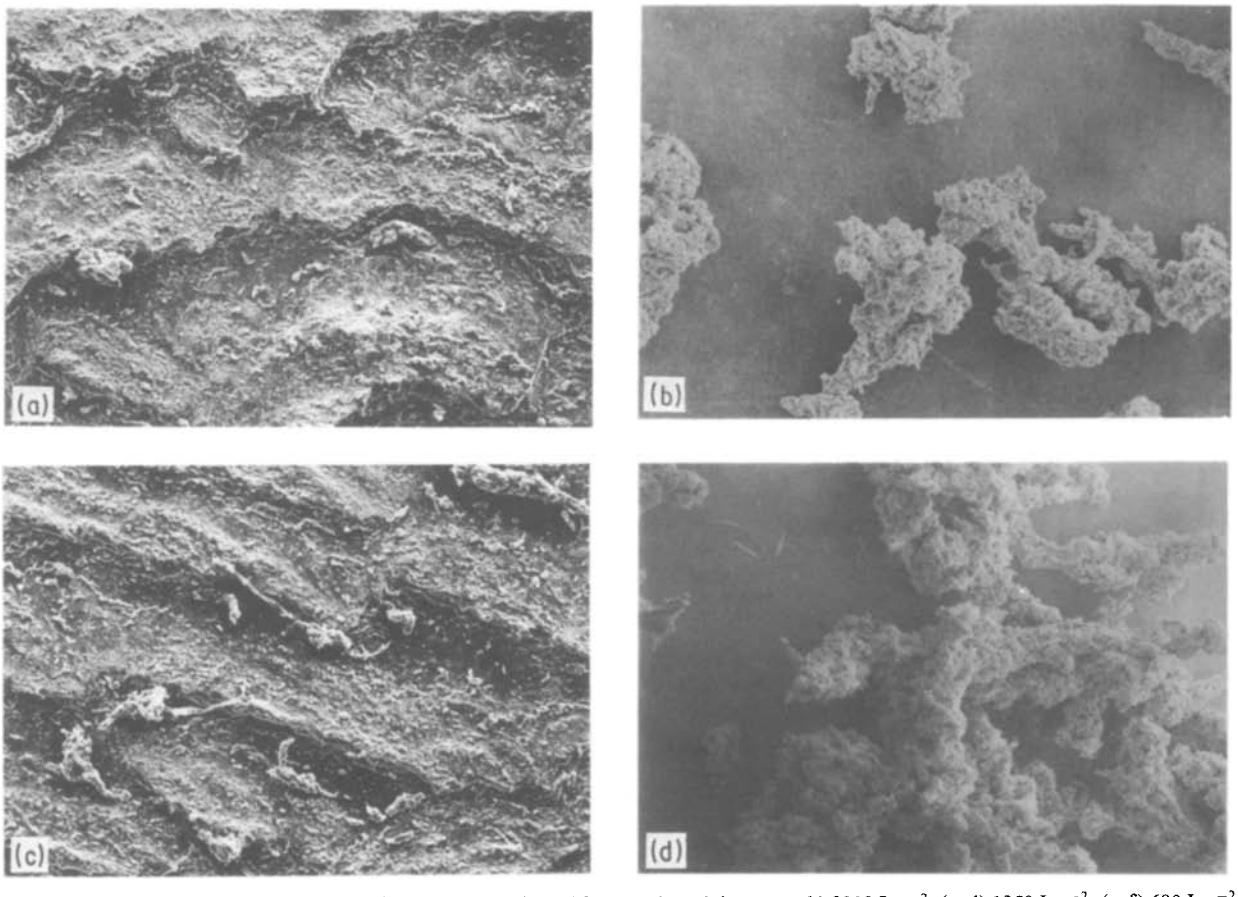

Figure 2 Natural rubber wear surfaces and debris as a function of frictional work input. (a, b) 2000 J m^{-2}, (c, d) 1350 J m^{-2}, (e, f) 690 J m^{-2}.

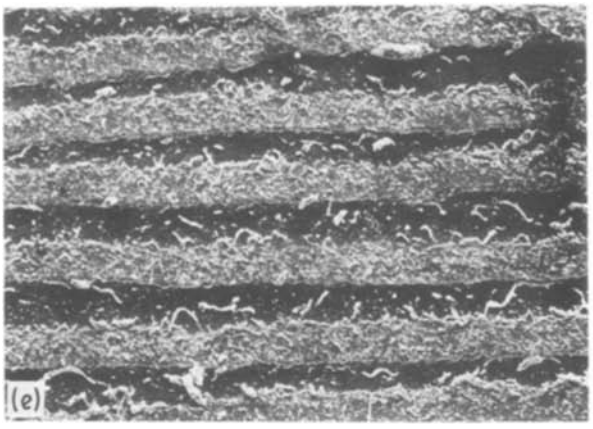

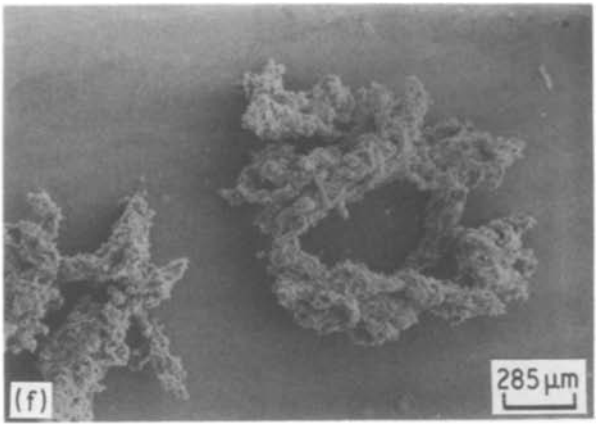

Figure 2 Continued.

Figure 3 Blend compound wear surfaces and debris as a function of frictional work input. (a, b) 2160 J m^{-2}, (c, d) 1430 J m^{-2}, (e) 730 J m^{-2}.

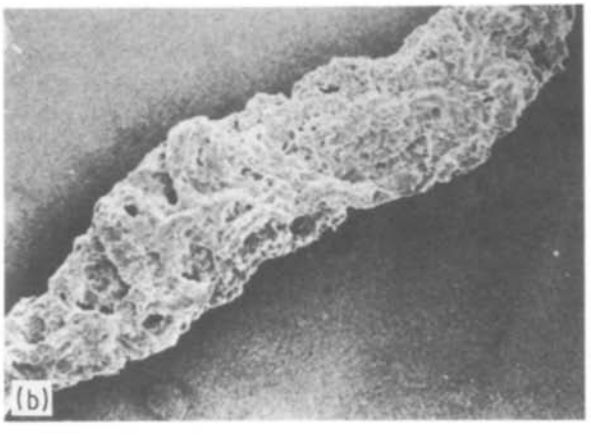

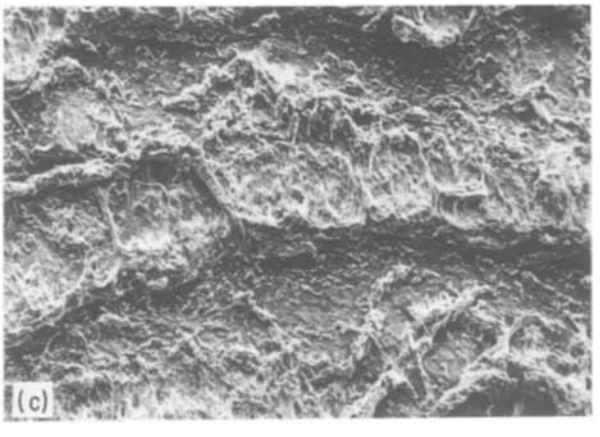

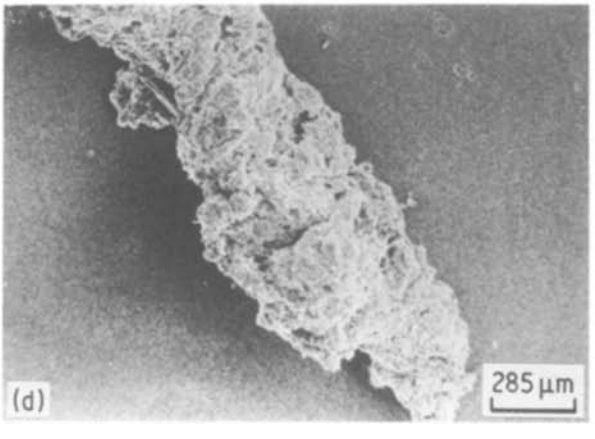

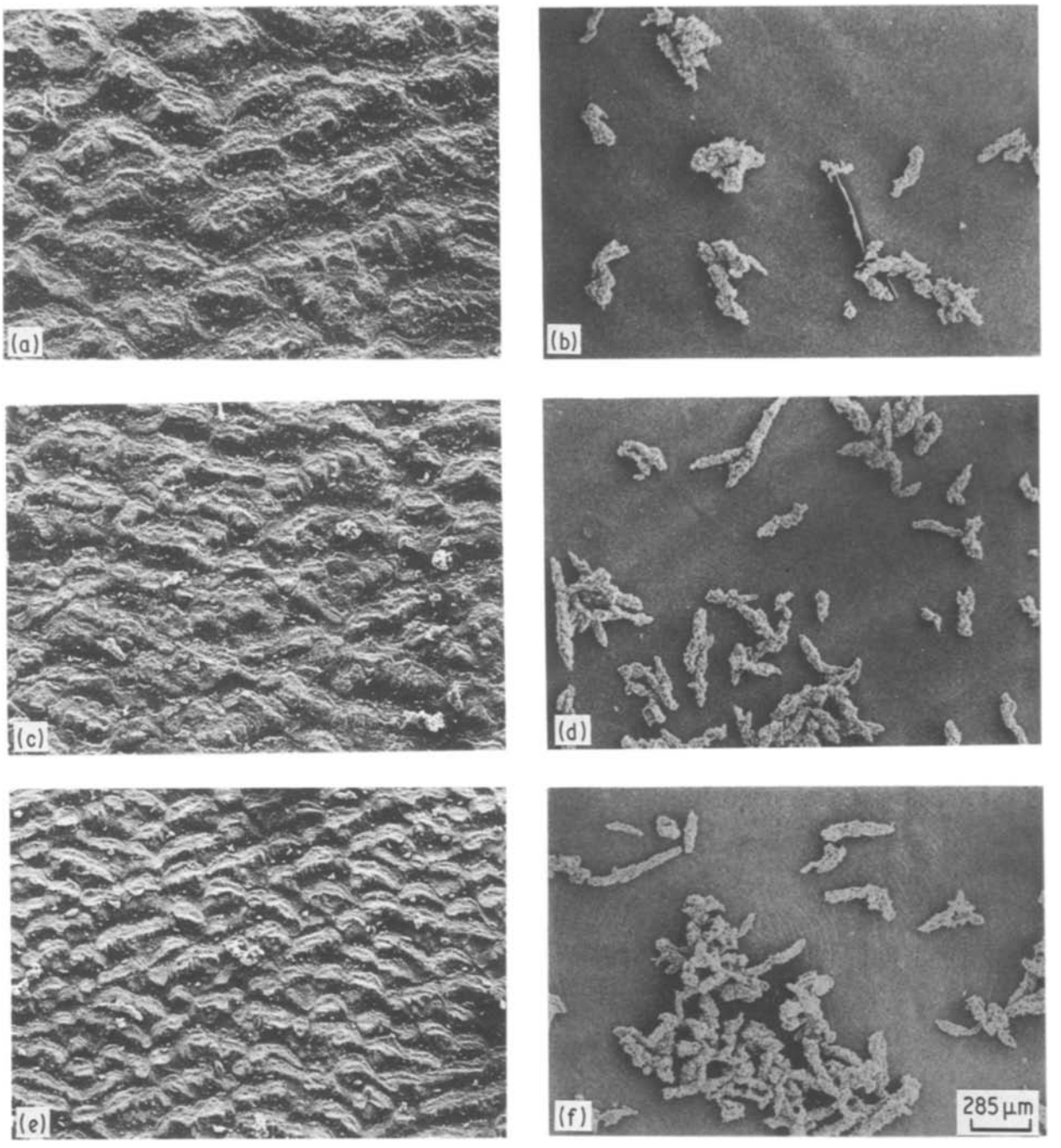

Figure 4 Polybutadiene rubber wear surfaces and debris as a function of frictional work input. (a, b) 1790 J m^{-2}, (c, d) 1220 J m^{-2}, (e, f) 650 J m^{-2}.

3.2. Analysis

The profilometer traces were mounted on 1 mm thick paper board. An Exacto-knife was used to cut along the rugged line. This produced a relief image of the trace. The relief was glued to a long sheet of paper where perimeter estimates were made by rolling discs of various diameters along the length of the trace edge. A hole in the centre of each disc allowed a pencil lead to record on the paper each path taken. Small discs conformed closely to the irregular outline, whereas large discs were unable to penetrate into many of the irregularities (Fig. 5). The length of each path was measured with an architect's scale, and was normalized by dividing by the projected length of the original profilometer trace. Measuring the profilometry trace

TABLE II Wear parameters A and n

Compound	A	n
NR	8.6×10^{-13}	1.83
Blend	2.0×10^{-12}	1.64
PBD	3.9×10^{-13}	1.65

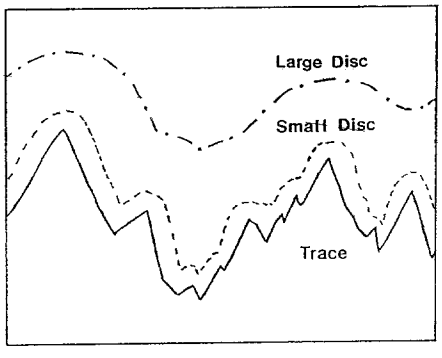

Figure 5 The effect of profilometer "radius" (disc diameter) on profilometer trace.

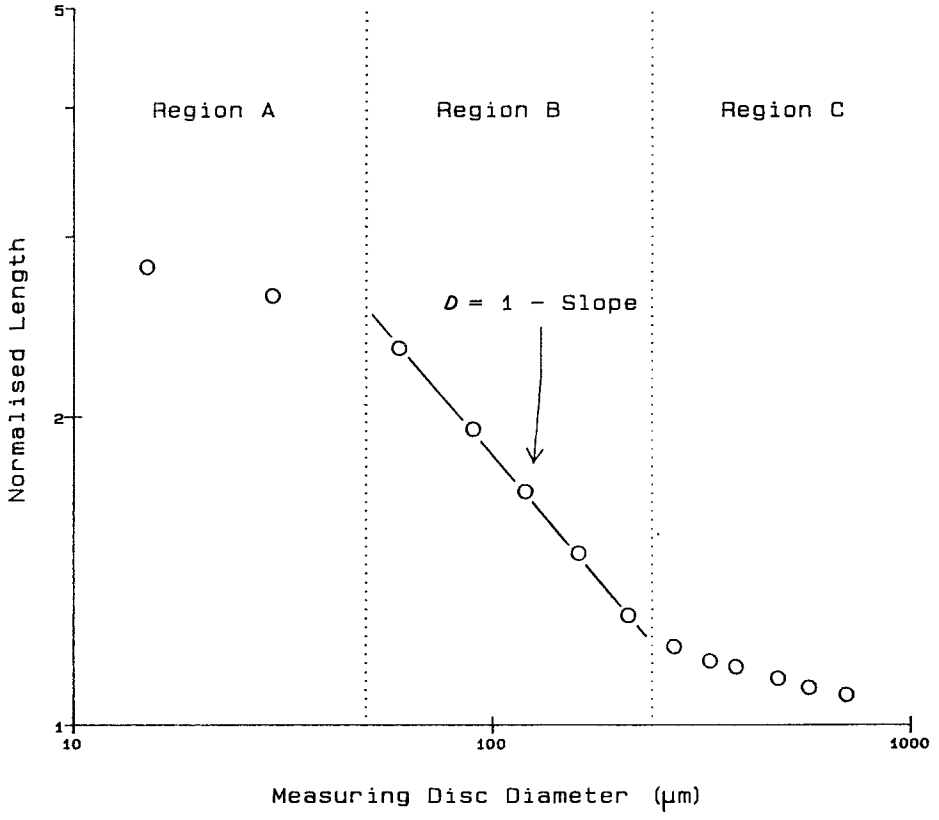

Figure 6 Typical fractal plot of profilometry data.

with discs is analogous to measuring surface roughness with a profilometer employing styli of different diameters [15].

3.3. Results and discussion

The fractal dimension of the surface traces was determined from the graphical representation of Equation 1, where L was the normalized length, the measuring unit R was the disc diameter, and the slope equalled $(1 - D)$. A typical result is shown in Fig. 6.

The fractal dimension was not constant over the entire range of measuring diameters because of the limited self-similarity of the wear surface. The graph was divided into three regions: A, B and C. As the disc size decreased in region A the path length approached the true length of the original stylus trace, whereas, in region C the surface features became less significant as the disc size increased. Therefore the fractal dimension in these zones decreased toward the Euclidean value $D = 1$. The fractal dimension was obtained from the approximately linear region B, Fig. 6. The resulting value is considered a meaningful descriptor of the surface because it applies to the range of disc sizes that correspond to the scale of the actual surface features.

TABLE III Fractal dimension of wear surfaces

Compound	Frictional work ($J m^{-2}$)	Fractal dimension
NR	2000	1.46
NR	1670	1.47
NR	1340	1.47
NR	690	1.32
Blend	2160	1.48
Blend	1750	1.49
Blend	1430	1.49
Blend	730	1.13
PBD	2080	1.55
PBD	1790	1.58
PBD	1220	1.52
PBD	650	1.51

Fractal plots as a function of frictional work input are shown in Fig. 7, and corresponding values of D are given in Table III. When compared with respect to the frictional work input, the measured fractal dimension values could be divided into two categories; constant over a work input range or deviant.

When D was constant with frictional work the curves could be superimposed over their entire lengths (regions A, B and C), by shifting the curves only along the measuring unit axis (Fig. 8). This demonstrates that although the fractal dimension was changing over the measuring size range, it changed at the same rate for each surface. The suggested physical interpretation of superposition is that the wear process creates surfaces that are morphologically similar except for a scale factor. This suggests that the same wear mechanism operates at each work input. In the case of the PBD material, this view is supported because PBD exhibits only dry wear. Oily wear does not occur because the reactive species generated during wear preferentially react with the bulk rubber, not with the oxygen present in the atmosphere [2]. Therefore, for these compounds, the fractal dimension and superposition could be used to identify similarities in wear mechanism.

The amount of shift required to superimpose the curves, the fractal shift factor ($\log S$), was related to the frictional work used to form the wear surfaces by

$$\log S = kF + b \quad (4)$$

where k is the slope and b is the intercept when the

reference fractal plot was the highest frictional work measured (Fig. 9). Rewriting this relation to make its physical meaning more apparent gives

$$F = K \log S + B \quad (5)$$

and noting that B is the reference frictional work. Then, if the reference frictional work is taken as zero, the equation becomes

$$F = K \log S \quad (6)$$

and the wear rate can be written as

$$W = A(K \log S)^n \quad (7)$$

Thus fractal analysis shows that the wear topography can be quantitatively relative to the wear rate. The values of log S and K for each material are listed in Table IV.

It is natural to note the similarity between the character of the fractal shift factor and the Williams, Landel and Ferry shift factor used to create master

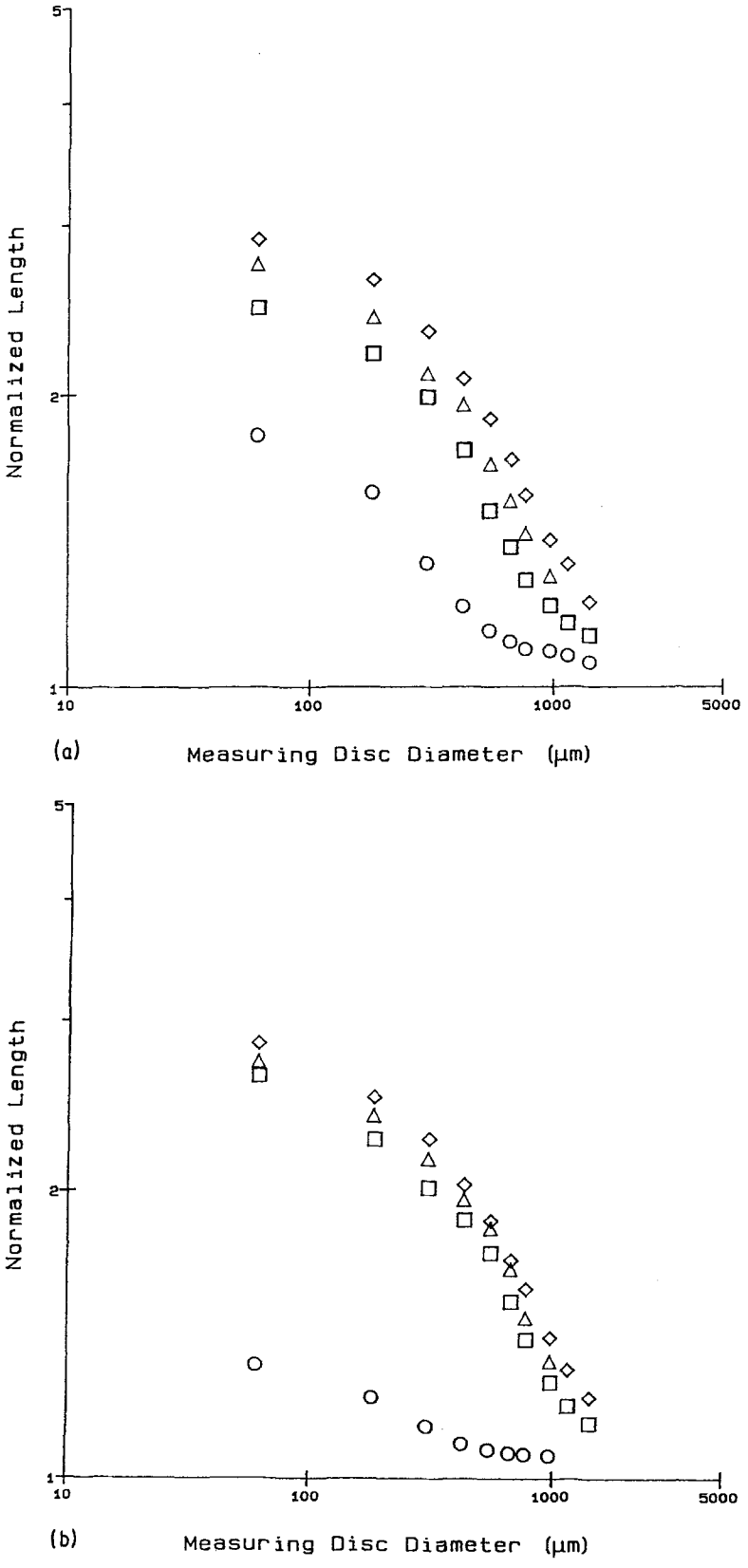

Figure 7 Fractal plot of profilometry data for (a) NR, (b) Blend, and (c) PBD compound. (a) (○) 690, (□) 1350, (△) 1670, (◇) 2000 J m^{-2}. (b) ○) 730, (□) 1430, (△) 1750, (◇) 2160 J m^{-2}. (c) (○) 650, (□) 1220, (△) 1790, (◇) 2080 J m^{-2}.

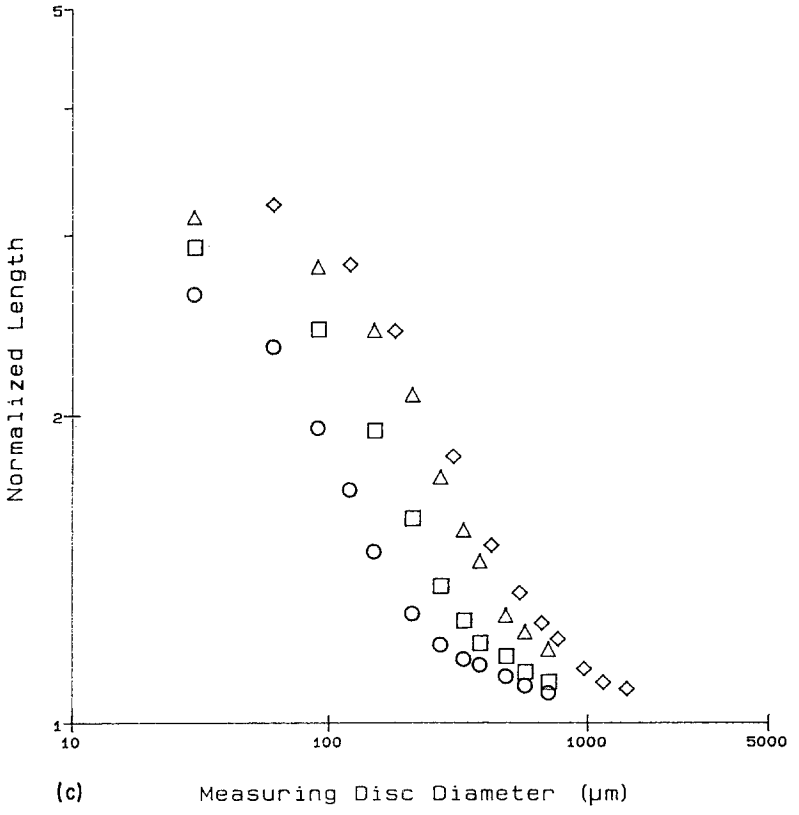

Figure 7 Continued.

curves of material behaviour controlled by viscous deformation. In fact, the ability to form master curves for wear rate as a function of load by taking in the account the rise in near surface temperature as a function of wear load has been demonstrated [6]. Efforts to correlate the fractal shift factor with near surface temperatures and wear load are in process.

However, the experimental results for the Blend and NR samples tested at reduced frictional work (690, 920 J m^{-2}, respectively), displayed lower dimension values than their neighbouring curves and superimposed only over a small region. This was due to a distinct change is surface morphology in both cases. The Blend transformed from dry wear at high frictional work to oily wear at low frictional work, while the surface of the NR material changed from a series of discontinuous, irregular ridges at high work inputs to small, uniformly spaced ridges at low work inputs. This change may be due to effects of strain crystallization [6] or the initiation of an oily mode transition.

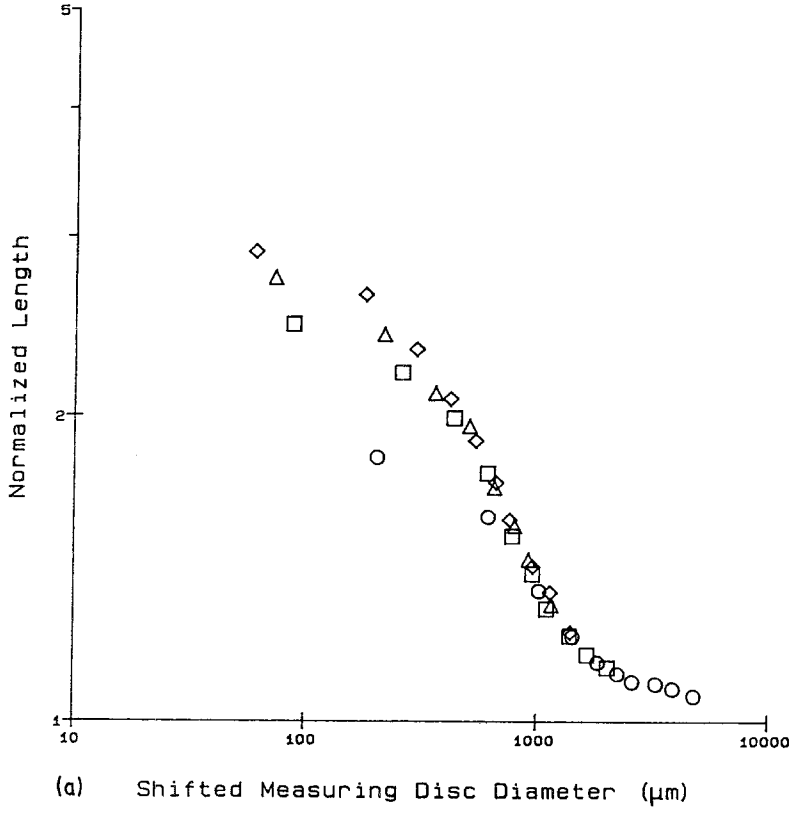

Figure 8 Shifted fractal plot for (a) NR, (b) Blend, and (c) PBD compound. (a) (○) 690, (□) 1350, (△) 1670, (◇) 2000 J m^{-2}. (b) (○) 730, (□) 1430, (△) 1750, (◇) 2160 J m^{-2}. (c) (○) 650, (□) 1220, (△) 1790, (◇) 2080 J m^{-2}.

Figure 8 Continued.

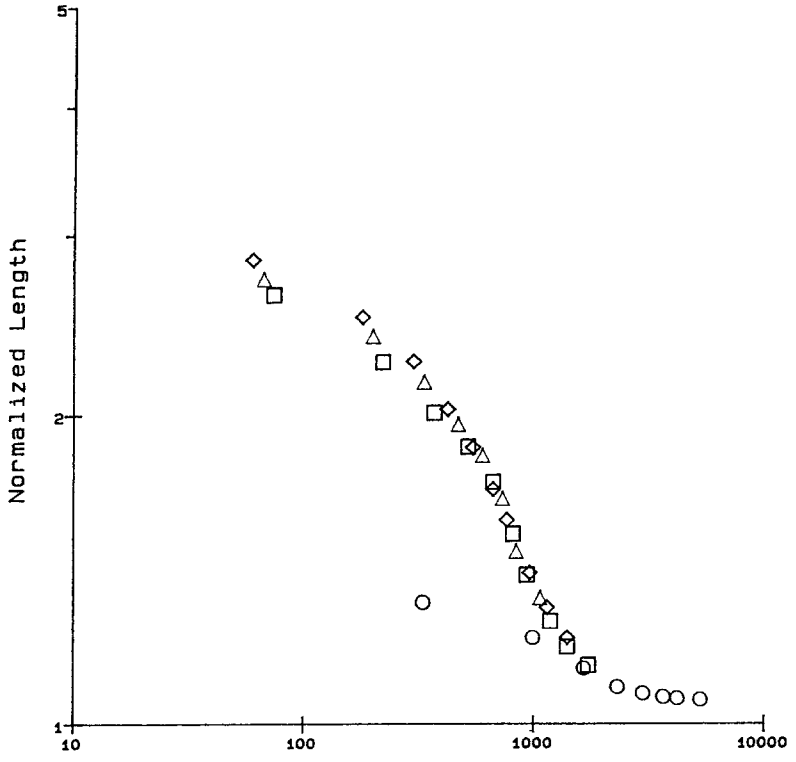

(b) Shifted Measuring Disc Diameter (μm)

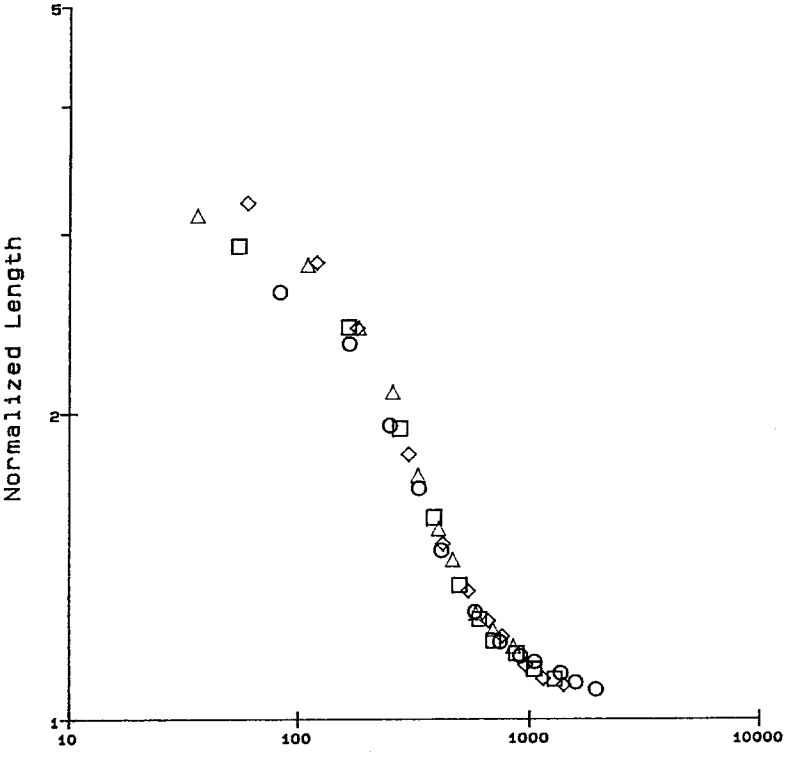

(c) Shifted Measuring Disc Diameter (μm)

The interpretation in both cases is that a change in the operative wear mechanism changes the fractal dimension and negates superposition.

These results show that although natural objects are not fractal over all scales, important practical information can be obtained from fractal analysis. The special ability of fractal analysis to describe a surface at all scales gives a complete topographic picture which can be effectively exploited through additional parameters such as the fractal shift factor. In brief, it is not necessary that a single fractal descriptor be found for every natural object. In fact, to attempt to do so would be equally as erroneous as promoting Euclidian geometry as a universal descriptor (i.e. mountains are not cones!) [10].

4. Wear debris

4.1. Experimental methods

Wear debris was collected for each surface analysed with profilometry except the oily mode specimen

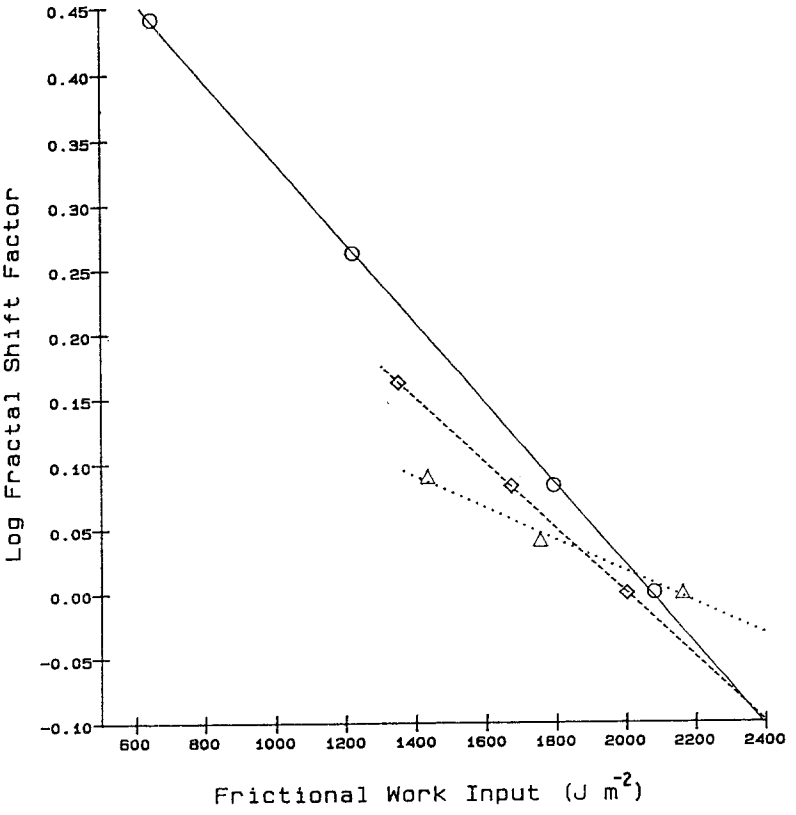

Figure 9 Log fractal shift factor as a function of frictional work input. (△) Blend, (◇) NR, (○) PBD.

which produced no debris. The particles were photographed in a scanning electron microscope at a fixed magnification. The micrographs were Xeroxed on to transparencies and projected onto a large sheet of heavy-weight paper where their boundary images were traced. The length of the irregular perimeter of each particle was measured with the architect's scale and the projected area was determined by weighing the particle image.

4.2. Results and discussion

The fractal dimension of the debris (D_d) was determined using Equation 4 relating the perimeter, P, to the projected area, A, found at a fixed magnification according to

$$P \propto A^{1/2D_d} \tag{8}$$

The data and D_d as a function of frictional work, are shown in Fig. 10 and Table V. A minimum of ten particle images were analysed to determine the fractal dimension of the debris at each frictional work input. For all materials tested, D_d for the debris increased with F (Fig. 11); for the NR and PBD compounds this can be expressed as

$$D = mF + 1 \tag{9}$$

where m equals 2 and $2.5 \times 10^{-10}\,m^2\,J^{-1}$ for the NR and PBD, respectively. However, for the blend the relation was not followed, apparently because the nature of the debris was radically different from NR and PBD. The blend debris was very sticky, adherent and cylindrical, rather than dry and particulate for the other compounds. Also, because of the sticky nature of the blend debris the size of the debris analysed only ranged over one order of magnitude, while the NR and PBD particles were significantly smaller and ranged over several orders of magnitude.

Currently it is thought that the physical origin of this expression is not related to the wear mechanism alone, but rather is a strong function of the scheme by which the debris is formed under the scraping action of the blade. In fact, the results from the wear surface

TABLE IV Log fractal shift factors for NR, Blend, and PBD compounds

Compound	Frictional work ($J\,m^{-2}$)	Log shift factor	K ($J\,m^{-2}$)
NR	2000 (Reference)	0.0000	
NR	1670	0.0828	−4000
NR	1350	0.1621	
NR	690	0.5310	
Blend	2160 (Reference)	0.0000	
Blend	1750	0.0414	−8330
Blend	1430	0.0897	
Blend	730	0.7379	
PBD	2080 (Reference)	0.0000	
PBD	1790	0.0828	−3230
PBD	1220	0.2621	
PBD	650	0.4414	

TABLE V Fractal dimension of NR, Blend, and PBD debris

Compound	Frictional work ($J\,m^{-2}$)	Fractal dimension
NR	2000	1.42 ± 0.04
NR	1340	1.24 ± 0.04
NR	690	1.12 ± 0.06
Blend	2160	1.36 ± 0.08
Blend	1430	1.14 ± 0.06
PBD	1790	1.44 ± 0.04
PBD	1220	1.34 ± 0.04
PBD	650	1.16 ± 0.04

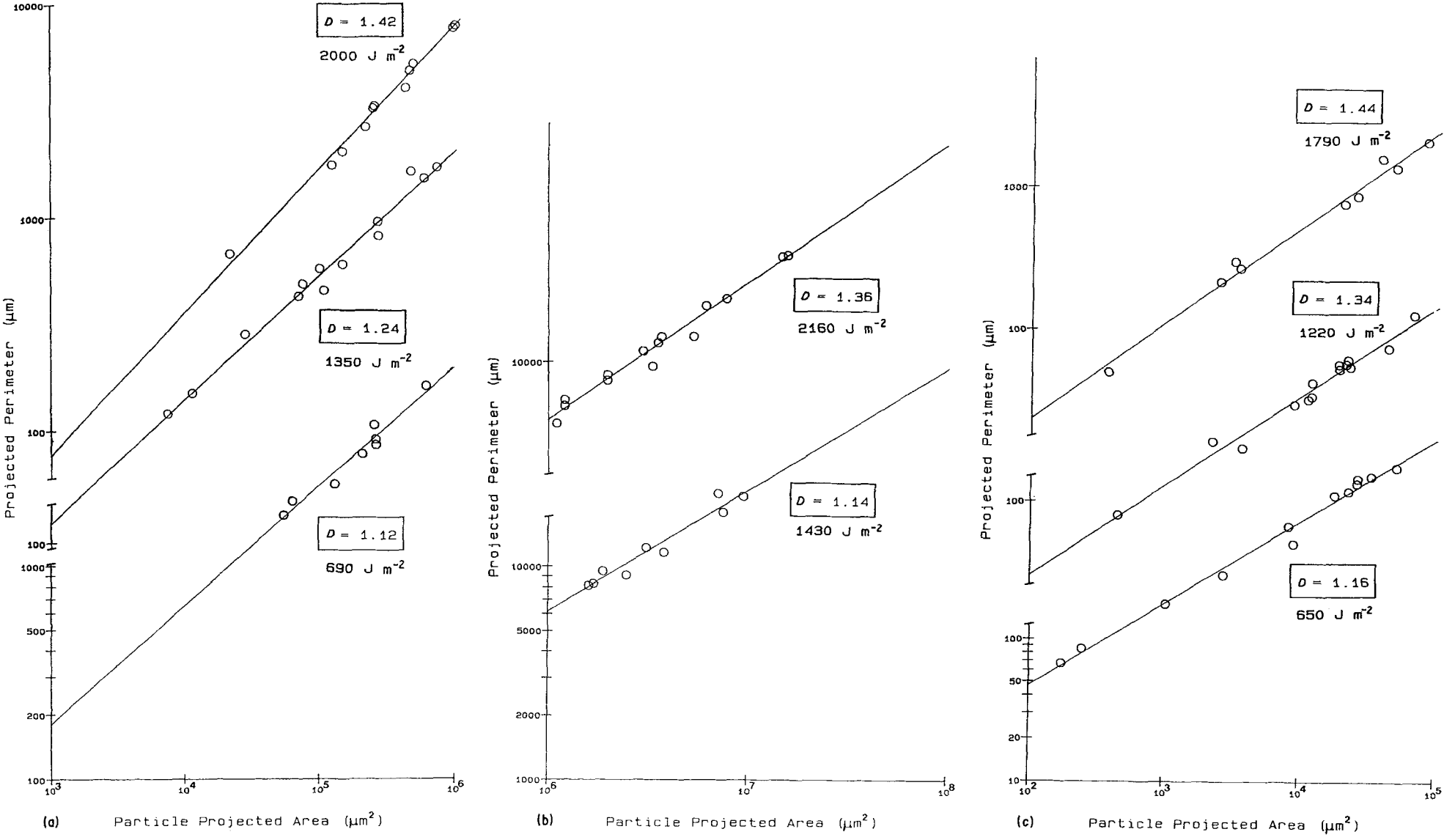

Figure 10 Fractal plots of (a) NR, (b) Blend, and (c) PDB debris.

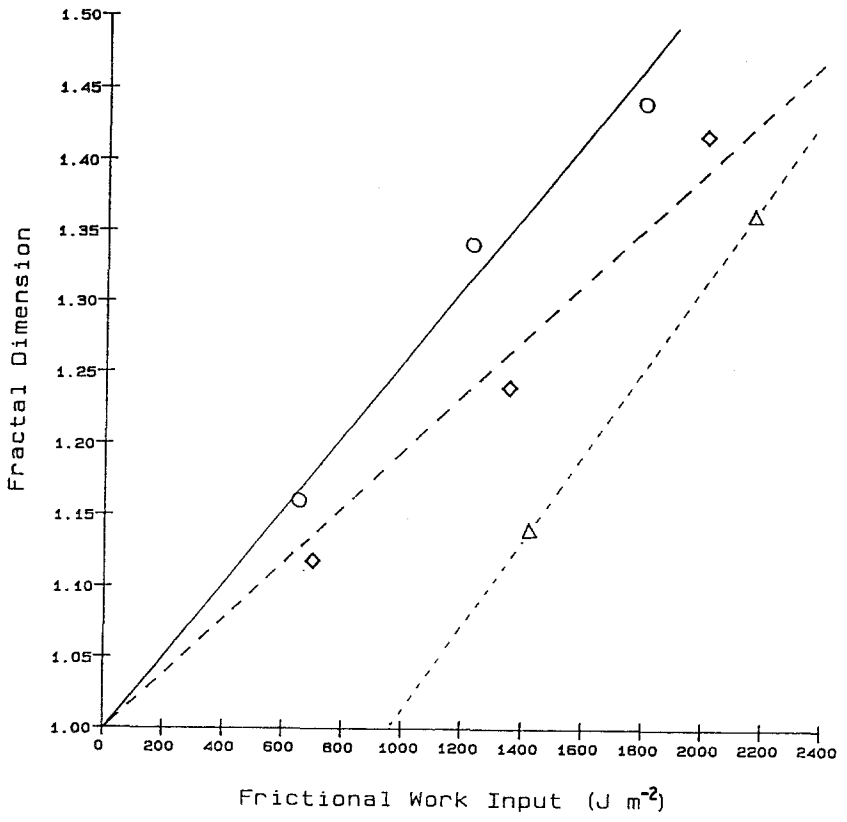

Figure 11 Fractal dimension of debris ad a functional work input. (△) Blend, (◇) NR, (○) PBD.

analysis indicates that over a large range of frictional work the surfaces are formed by the same mechanism. Therefore, if the debris was formed solely by this mechanism, its fractal dimension would be expected to have the same value!

It is proposed that at increasing wear rates more debris particles, which consist of primary particles and severed ridge tips, are produced per revolution and agglomerate with each pass of the blade until they are eventually removed. It is also believed that the detailed agglomeration mechanism is a function of the frictional work and responsible for the variation in the fractal dimension. A large body of information exists regarding the application of fractals to computer simulated random flocs in two and three dimensions [16–18]. Further interpretation of the precise agglomeration process would logically begin there.

Another feature of large random accreations of particles is an extensive range of self-similarity. This is evident from the many magnitudes over which the fractal dimension describes the rubber debris. This is further demonstrated in Fig. 12, where micrographs of the same debris particle continue to reveal more detailed irregularities with increasing magnification.

5. Conclusions

The dimension of rubber wear surfaces was fractal over a limited scale, and if the wear mechanism remained the same then the fractal plots could be superimposed. The required fractal shift factor was linearly related to the wear load. The fractal shift factor is highly suggestive of the classic WLF shift factor that relates viscous deformation processes to material properties. This relation is the focus of future research.

The wear debris was fractal and its dimension also increased with the wear load, but because the debris are agglomerates of wear particles the relation to wear load is thought to result from the effect of the wear load on the agglomeration mechanism.

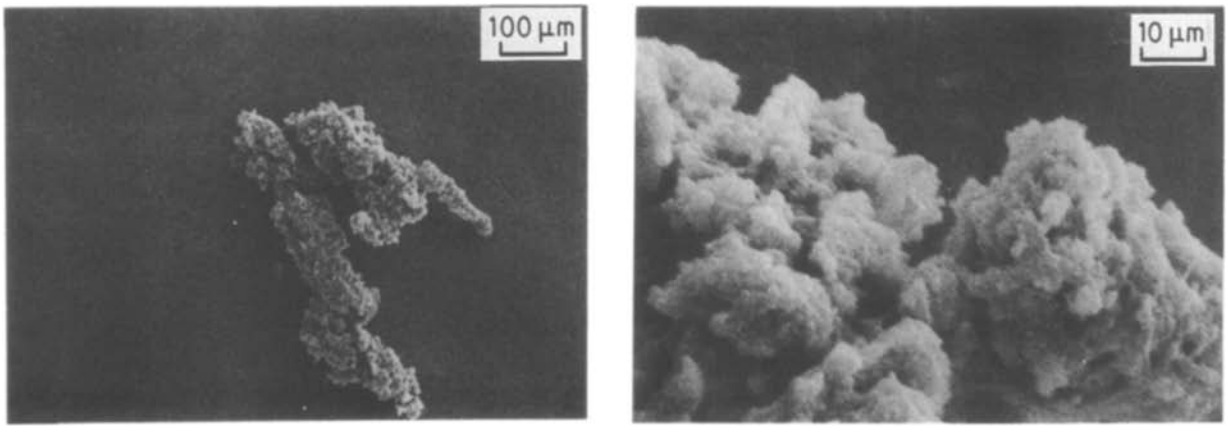

Figure 12 Self-similarity of debris particles.

Acknowledgements

The financial support of the US Army Research Office, Durham, is gratefully acknowledged and appreciated. We also thank P. Touchet and G. Rodriguez, US Army Belvoir R and D Center for supplying the materials.

References

1. M. L. DANNIS, *Rubber Chem. Technol.* **47** (1974) 1011.
2. A. N. GENT and C. T. R. PULFORD, *J. Appl. Polym. Sci.* **28** (1983) 943.
3. E. M. DANNENBURG, *Rubber Chem. Technol.* **59** (1986) 497.
4. V. I. DYRDA, V. I. VETTEGREN and V. P. NADUTYI, *Int. Polym. Sci. Technol.* **3** (1976) 26.
5. R. W. SMITH and A. G. VEITH, *Rubber Chem. Technol.* **55** (1982) 469.
6. A. SCHALLAMACH, *ibid.* **41** (1968) 209.
7. A. G. THOMAS, *ibid.* **48** (1974) 902.
8. E. SOUTHERN and A. G. THOMAS, *ibid.* **52** (1979) 1008.
9. S. W. ZHANG, *ibid.* **57** (1984) 755.
10. B. B. MANDELBROT, "The Fractal Geometry of Nature" (Freeman, New York, 1982).
11. S. LOVEJOY, *Science,* **216** (1982) 185.
12. B. B. MANDELBROT, D. E. PASSOJA and A. J. PAULLAY, *Nature* **308** (1984) 721.
13. C. S. PANDE, L. R. RICHARDS and S. SMITH, *J. Mater. Sci. Lett.* **6** (1987) 295.
14. E. F. UNDERWOOD and K. BANERJI, *Mater. Sci. Engng* **80** (1986) 1.
15. D. FARIN, S. PELEG, D. YAVIN and D. AVNIR, *Langmuir* **1** (1985) 399.
16. P. MEAKIN, *J. Coll. Int. Sci.* **96** (1983) 415.
17. P. MEAKIN and Z. R. WASSERMAN, *Chem. Phys.* **91** (1984) 392.
18. R. C. BALL and T. A. WITTEN, *J. Stat. Phys.* **36** (1984) 873.

Received 27 July
and accepted 23 October 1987